Energy

DC-DC Converter Implementations Based on Piezoelectric Resonators

J. D. Boles, J. J. Piel, D. J. Perreault
Sponsorship: Texas Instruments, NSF Graduate Research Fellowship, MASDAR

Power electronics play a vital role in the technological advancement of transportation, energy systems, manufacturing, healthcare, information technology, and many other major industries. Demand for power electronics with smaller volume, lighter weight, and lower cost often motivates designs that better utilize a converter's energy storage components, particularly magnetics. However, the achievable power densities of magnetic components inherently reduce as volume decreases, so further progress in converter miniaturization will eventually require new energy storage mechanisms with fundamentally higher energy density and efficiency capabilities.

This prompts investigation into piezoelectric energy storage for power conversion; piezoelectrics have comparatively superior volume scaling properties. While piezoelectrics have been used extensively for sensing, actuation, transduction, and energy harvesting applications, their adoption in power conversion has been more limited. Converter designs based on single-port piezoelectric resonators (PRs) report limited power and/or performance capability, but without investigation into the full realm of possible converter implementations.

In this work, we conduct a systematic enumeration and downselection of practical dc-dc converter switching sequences and topologies that best leverage PRs as their only energy storage components. In particular, we focus on switching sequences that facilitate high-efficiency behaviors (e.g., low-loss resonant charging/discharging of the PR's input capacitance and all-positive instantaneous power transfer) with voltage regulation capability. To analyze and compare implementations, we demonstrate methods for mapping PR state trajectories across a switching cycle, imposing practical constraints on PR behavior, evaluating PR utilization, and estimating PR efficiency.

Effective use of the PR's resonant cycle enables these converter implementations to achieve strong experimental performance with peak efficiencies >99%, even with presently commercially-available PRs. This suggests that these PR-based converters are promising alternatives to those based on traditional energy storage. With further development, PR-based converters may pave the way for high-performance converter miniaturization in applications spanning consumer electronics, biomedical implants, and flight.

(a)
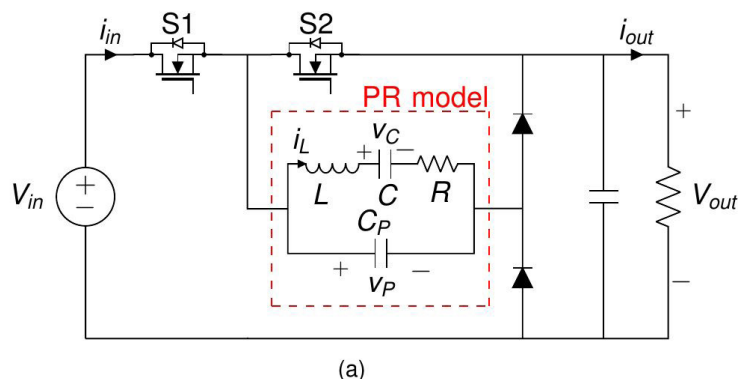
▲ Figure 1: Schematic of one PR-based converter topology, which relies on only the PR for energy storage and has only two active switches.

(b)
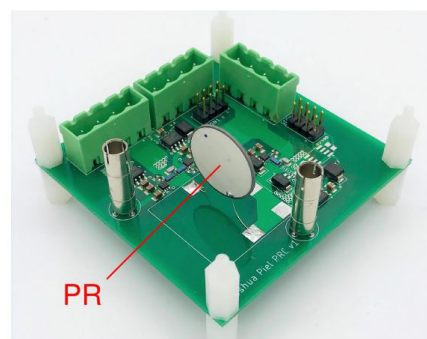
▲ Figure 2: Photograph of a converter prototype corresponding to this schematic.

FURTHER READING

- J. D. Boles, J. J. Piel, and D. J. Perreault, "Enumeration and Analysis of Dc-dc Converter Implementations Based on Piezoelectric Resonators," in Proc. *IEEE Workshop on Control and Modeling for Power Electronics*, Toronto, Canada, Jun. 2019, pp. 1–8.
- J. D. Boles, J. J. Piel, and D. J. Perreault, "Analysis of High-efficiency Operating Modes for Piezoelectric Resonator-based Dc-dc Converters," in Proc. *IEEE Applied Power Electronics Conference and Exposition*, New Orleans, LA, USA, Mar. 2020, pp. 1–8.
- C.-S. Kim, S. R. Bishop, and H. L. Tuller, "Electro-chemo-mechanical Studies of Perovskite-structured Mixed Ionic-electronic Conducting SrSn$_{1-x}$Fe$_x$O$_{3-x/2+\delta}$ Part I: Defect Chemistry," *J. Electroceram.*, vol. 38, pp. 74-80, 2017.

High Capacity CMOS-compatible Thin Film Batteries

M. J. Chon, A. Weathers, M. Polking, J. Kedzierski, H. Chea, X. Wang, P. Kumar, L. Racz, C. V. Thompson
Sponsorship: Lincoln Laboratory

The miniaturization of sensors through advancements in low-powered MEMS devices in integrated circuits has opened up new opportunities for thin film microbatteries. However, many of the available thin film battery materials require a high-temperature process that necessitates additional packaging volume, which reduces the overall energy density of these batteries. Previous research with collaborators in Singapore demonstrated an all-solid-state materials system with high volumetric capacity that exclusively utilizes CMOS-compatible (i.e., room temperature) processes. This process allows integration of these batteries directly onto CMOS circuits, thereby achieving energy densities comparable to bulk batteries for applications in distributed power supplies and integrated autonomous microsystems (Figure 1).

Additionally, the ability to deposit all components of the battery at room temperature makes it possible to fabricate these batteries on thin, flexible substrates that can be densely stacked to achieve a wide range of capacities without sacrificing their high energy density.

We have successfully demonstrated a full thin film microbattery using Ge and RuO_2 as anode and cathode materials, respectively, with LiPON as the solid-state electrolyte (Figure 2b). Although RuO_2 has traditionally been used as an anode material, it has significantly higher volumetric capacity than typical cathode materials and sufficiently high electrochemical potential versus Ge to provide an output voltage of ~ 0.5V at a capacity of ~40 Ah/cm³ (Figure 2a).

▲ Figure 1: Schematic of thin film battery fabricated on top of autonomous sensor. CMOS-compatibility allows direct integration with underlying integrated circuit. Battery provides power to sensor and stores energy from integrated harvester.
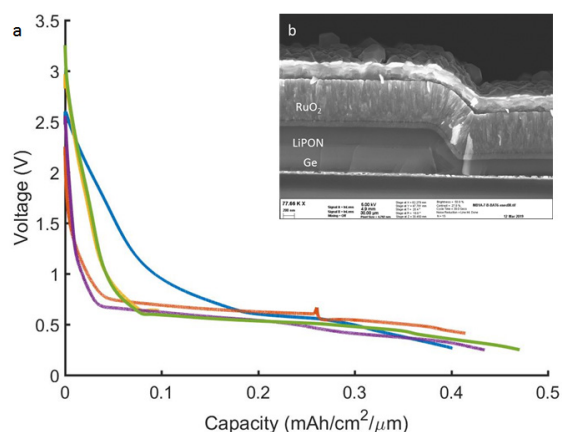
▲ Figure 2: (a) Voltage profile of full battery during discharge. (b) Scanning electron microscope image showing components of solid-state microbattery. Layers of LiPON and RuO_2 were sputter-deposited, allowing them to fully conform over edge of Ge anode.

FURTHER READING

• D. Perego, J. S. T. Heng, X. Wang, Y. Shao-Horn, C. V. Thompson, "High-performance Polycrystalline RuOx Cathodes for Thin Film Li-ion Batteries," *Electrochimica Acta*, vol. 283, pp. 228-233, Sept. 2018.

State Estimation, Parameter Inference, and Observability Analysis of Electrical Distribution Networks

M. J. Chon, A. Weathers, M. Polking, J. Kedzierski, D. Nezich, H. Chea, L. Racz, C. V. Thompson
Sponsorship: Lincoln Laboratories

In modern electrical power systems, distribution networks facilitate the final step of power delivery to homes and businesses. Distributed energy resources (DERs) such as Tesla powerwalls and rooftop PV systems, automated sensing devices equipped with telemetry capabilities such as micro-Phasor Measurement Units (μ-PMUs) and smart meters, and active loads, which are capable of responding to real-time pricing signals, all significantly disrupt the standard operating procedures of distribution networks. One of the primary roadblocks to successful operation and control of these systems is the lack of network observability. Due to the significant cost and effort associated with sensor deployment in ultra-large distribution networks, system operators must alternatively leverage the physical model of the network and various measurement sets to reconstruct the so-called "state" (i.e., voltage equilibrium) of the network. State estimation, therefore, is a vitally important tool for distribution system operators. Because network parameter values span many orders of magnitude and sensors are critically under-deployed, the traditional state estimation problem is severely ill-conditioned and is seldom deployed in the field.

Standard DSSE techniques rely on strong, yet potentially unjustified, regularization to combat the ill-conditioning of the problem. In this project, we represent the operation of a distribution system as a sequence of nonlinear maps that relate measurements, states, controller decisions, and operational performance. Using advanced uncertainty quantification techniques, we quantify the subspace of input perturbations whose response is practically "unobservable" at the output of each nonlinear map. These sensitivity results (which must be regathered each time state estimation is employed) guide the selection of appropriate regularization methods whose application can be probabilistically justified. We therefore carefully apply varying degrees of statistical regularization, such as Bayesian priors, and physics-based regularization to solve the state estimation problem. Further uncertainty quantification not only gauges the quality of the result, but also suggests optimal field testing and optimal placement of future deployed sensors to system operators.

Despite regularization, the Hessian used to iteratively solve the state estimation problem can still exhibit severe numerical ill-conditioning. To overcome this numerical ill-conditioning, we are developing a set of computationally efficient and numerically robust methods to invert the Gauss-Network "gain" matrix. This solution utilizes a semi-explicit LU decomposition in conjunction with a matrix series expansion (i.e., Neuman expansion) and sequential applications of the so-called Woodbury matrix identity. Homotopy methods are used to scale the measurement variances and line lengths to decrease the number of iterations needed to converge on a final solution.

FURTHER READING

- M. Vadari, "The Future of Distribution Operations and Planning: The Electric Utility Environment Is Changing," *IEEE Power and Energy Magazine, vol. 18, no. 1, pp. 18-25,* Jan.-Feb. 2020.
- Primadianto and C.N. Lu, "A Review on Distribution System State Estimation," *IEEE Transactions on Power Systems*, vol. 32, no. 5, pp. 3875–3883, Sep. 2017.

Maximizing the External Radiative Efficiency of Hybrid Perovskite Solar Cells

D. W. deQuilettes, M. Laitz, R. Brenes, B. Dou, B. T. Motes, S. D. Stranks, H. J. Snaith, V. Bulović, D. S. Ginger
Sponsorship: Tata Trusts

Despite rapid advancements in power conversion efficiency (PCE)in the last decade, perovskite solar cells still perform below their thermodynamic efficiency limits. Non-radiative recombination, in particular, has limited the external radiative efficiency and open circuit voltage in the highest performing devices. We review the historical progress in enhancing perovskite's external radiative efficiency (ERE) and determine key strategies for reaching high optoelectronic quality. Specifically, we focus on non-radiative recombination within the perovskite layer and highlight novel approaches to reduce energy losses at interfaces and through parasitic absorption. If defects are strategically targeted, it is likely that the next set of record-performing devices with ultra-low voltage losses will be achieved.
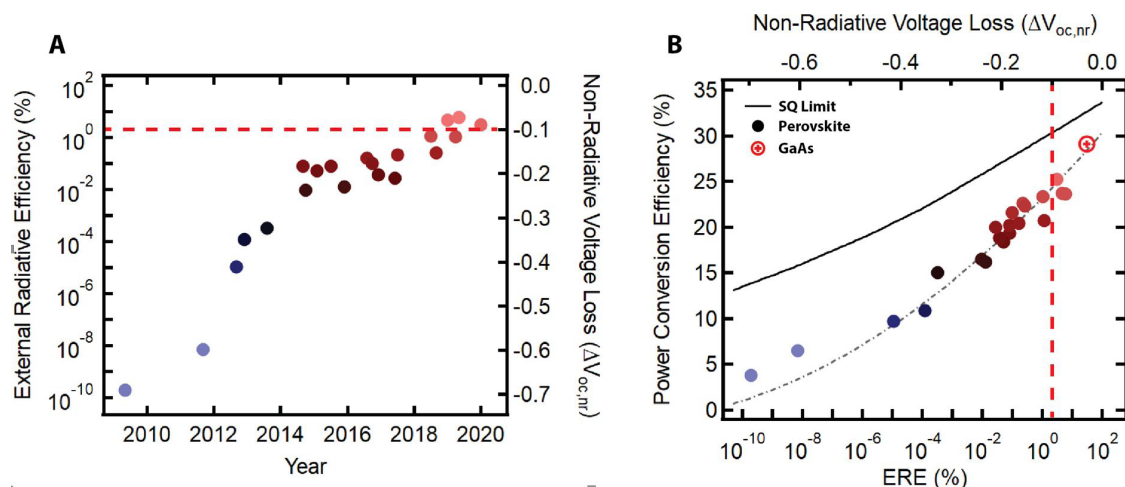
▲ Figure 1: (A) ERE and non-radiative voltage loss of a selection of pioneering perovskite devices work as a function of publication date. The red dashed line represents the threshold for achieving the next set of high ERE and low voltage loss devices. (B) Plot of perovskite PCE versus ERE and non-radiative voltage loss along with a nonlinear trendline (dashed black line) and the record GaAs solar cell. The black solid line shows the Shockley-Queisser (SQ) maximum theoretical PCE irrespective of material bandgap.

FURTHER READING

- D. W. deQuilettes, M. Laitz, R. Brenes, B. Dou, B. T. Motes, S. D. Stranks, H. J. Snaith, V. Bulović, and D. S. Ginger, "Maximizing External Radiative Efficiency of Hybrid Perovskite Solar Cells," *Pure Appl. Chem.*, 2020.

Blade Coating of Perovskite Solar Cells Toward Roll-to-roll Manufacturing

B. D. Dou, V. Bulović
Sponsorship: Tata Trusts

High efficiency combined with transformative roll-to-roll (R2R) printability makes metal halide perovskite-based solar cells the most promising solar technology to address the terawatt challenge of the future energy demand. However, translation from lab-scale deposition solution processing techniques, such as spin coating, to large-scale R2R compatible methods has been a significant challenge due to fundamental differences in coating fluid dynamics and resulting drying and crystallization processes with the different coating methods. Here we address this challenge by developing processes and device architectures with high-speed (> m min-1) blade-coating (Figure 1A), which is R2R manufacturing compatible. We constructed solar cells with structure of Glass/FTO/SnO2/ FA0.8MA0.16Cs0.04PbBr0.16I0.84/Spiro-MeOTAD/ MoOX/Ag (Figure 1B), where the SnO2 is blade-coated at an environment of 49% relative humidity and with overall device thickness of less than 1 μm, excluding the glass substrate. We demonstrated a light-to-electricity conversion efficiency up to 17%, with open-circuit voltage of 1.112 V, short-circuit current of 22.12 mA cm-2, and fill factor of 69.1% (Figure 1C). The application of blade-coating of SnO2 has been a first step to show the potential of scaling highly efficient perovskite solar cells with transformative R2R compatible manufacturing techniques.
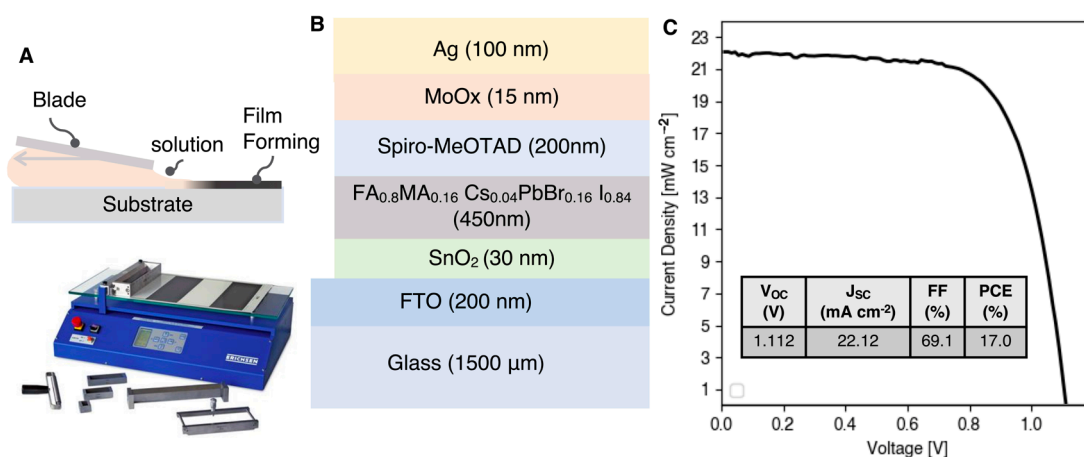
▲ Figure 1: (A) Schematic of blade coating process and blade coater. (B) The solar cell device architecture applied in this study. (C) A typical device's current density–voltage characteristics.

Solid State Batteries: Interfacial Degradation Between Solid Electrolyte and Oxide Cathodes

Y. Kim, A. Rahman, B. Yildiz
Sponsorship: ISN, Ford Motor Company

All-solid-state batteries (SSBs) promise safer and higher performance energy storage than the present liquid-electrolyte Li-ion batteries. $Li_7La_3Zr_2O_7$ and $Li_{1+x}Al_xTi_{2-x}(PO_4)_3$ are promising solid electrolytes for Li-ion SSBs. The wide electrochemical window of $Li_7La_3Zr_2O_7$ enables usage of a Li metal anode and high-voltage oxide cathodes. This combination makes $Li_7La_3Zr_2O_7$ a promising candidate for a high-capacity battery cell. $Li_{1.4}Al_{0.4}Ti_{1.6}(PO_4)_3$ has a high stability window and excellent chemical stability against moisture, enabling large-scale production with minimal cost. However, the development of SSBs in both systems is hindered mainly due to the high cathode |electrolyte interfacial resistance, which impedes the Li-ion transfer and ultimately the durability and power density. Sintering, which is necessary to get good contact between a cathode and an electrolyte, leads to the formation of detrimental phases that are insulting for Li-ion transfer. Despite the importance of the issue, only limited understanding of the interfacial chemistry exists so far. The lack of research comes from the challenges in investigating buried interfaces.

We aim to advance the understanding and control over the stability of the cathode|electrolyte interfaces. We use model systems made of thin-film cathode layers on dense electrolyte pellets (Figure 1). This approach enables us to use surface-sensitive and non-destructive techniques such as X-ray absorption near edge spectroscopy (XANES) and extended X-ray absorption fine structure (EXAFS) to study buried interfaces. Our findings show that interfacial degradation is highly dependent on the gas environment used in the sintering process (Figure 2). Annealing in O_2 environment does not lead to formation of a detrimental phase at the interface. In contrast, annealing in air or in CO_2 led to severe degradation. We attribute this to the formation of Li_2CO_3 and delithiated phases at the interface. The findings from this project will lead to identifying suitable process parameters to develop a stable cathode-electrolyte interface with good electrochemical properties.
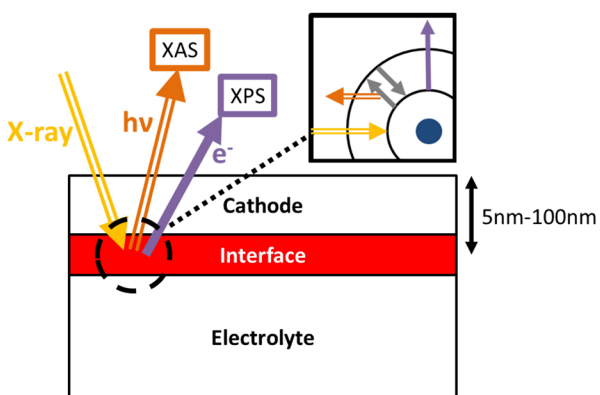
▲ Figure 1: Sample design to study buried interface. Thin film (5nm-100nm) cathode is used so interfacial region is within detection depth of surface sensitive techniques (XAS, XPS).
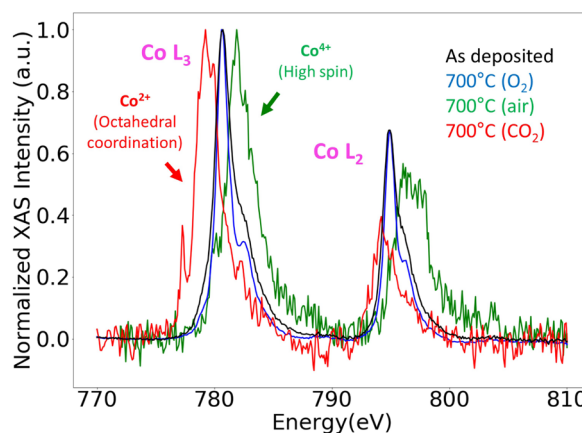
▲ Figure 2: Chemical stability comparison at $LiNi_{0.6}Mn_{0.2}Co_{0.2}O_2|Li_7La_3Zr_2O_{12}$ interface after annealing at 700°C, 4h in O_2, air and CO_2 shown by Co L-edge XAS. Annealing in air or CO_2 leads to drastic change of oxidation state due to secondary phase formation.

FURTHER READING

- P. Žguns, G. Vardar, Y. Kim, W. Bowman, Y-M. Chiang, and B. Yildiz, "Chemical and Electrochemical Stability at Electrode Surfaces and Electrode-Electrolyte Interfaces," presented at *22nd International Conference on Solid State Ionics*, PyeongChang, Korea, 2019.
- Y. Kim, G. Vardar, Y-M. Chiang, and B. Yildiz, "Structure, Chemistry and Charge Transfer Resistance of the Interface Between Garnet Solid Electrolyte and Oxide Cathodes," p*resented at 2019 MRS Fall Meeting & Exhibit*, Boston, MA, U.S.A., 2019.

Techno-economic Assessment and Deployment Strategies for Vertically-mounted Photovoltaic Panels

A. Panda*, R. Zimmerman*, V. Bulović
(*Equal Contributors)
Sponsorship: Tata Trusts, American Tower Corporation

Conventional schemes of panel mounting require horizontal space, on the order of 20,000 to 40,000 m² per megawatt peak (MW$_p$), prompting us to investigate new strategies for deploying solar panels. Mounting solar photovoltaic (PV) panels vertically to the sides of existing structures, such as facades of buildings, offers one such strategy. Vertically-mounted PVs take advantage of otherwise unused vertical real estate in the built environment, with minimal additional structural reinforcement costs and no need for additional land area use. Uniquely, the peak electricity generation time of west-facing vertically-mounted PV panels occurs closer to the hour of maximum consumer power demand, allowing increased electricity generation when the same PV panels, if conventionally mounted, would generate lower amounts of power.

Keeping these advantages in mind, we identified a set of potential profitable markets in the United States (U.S.) and enumerated the technical challenges to expanding PV usage into these markets. We calculated the levelized cost of electricity (LCOE) for vertically-mounted PVs as a function of the azimuth panel; then using county-level resolution we estimated economic viability for these installations in the contiguous U.S. The LCOE calculations allow us to identify target specifications for vertical PV panels to be economically competitive when compared to the commercial grid electricity. We show that lightweight, flexible and bifacial form factors attainable with the next-generation PV technology can lead to installation cost reductions. We are developing roof-of-concept prototypes to validate our hypothesized deployment strategies.
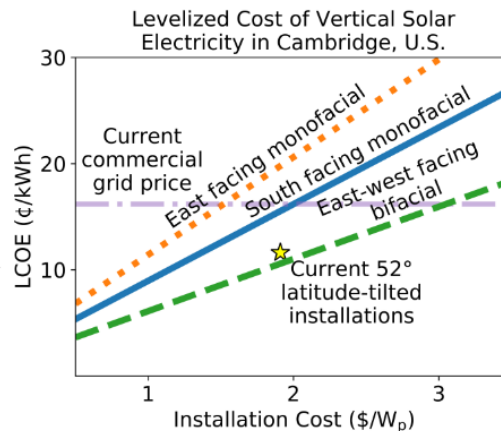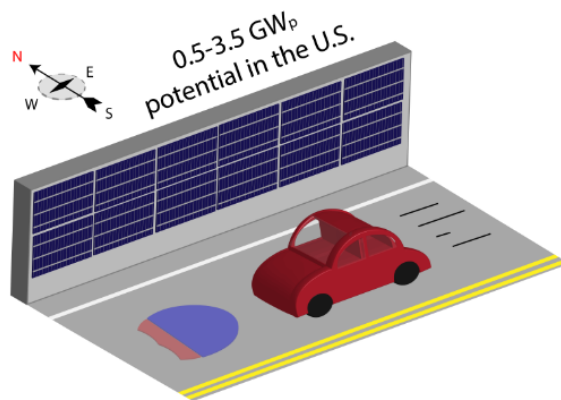
▲ Figure 1: Visual representation of one potential vertically-mounted PV panel market as a sound barrier for the US interstates (left). The cost of commercial grid electricity in Cambridge, and the LCOE from vertically-mounted PV panels as a function of azimuth and installation cost (right).

Silicon MEMS Compatible Bipropellant Micro Rocket Engine Using Steam Injector

J. Protz
Sponsorship: Protz Lab Group; microEngine, LLC; Asteria Propulsion, LLC

Rocket engines miniaturized and fabricated using MEMS or other techniques have been an active area of research for two decades. At these scales, miniaturized steam injectors like those used in Victorian-era steam locomotives are viable as a pumping mechanism and offer an alternative to pressure feed and high-speed turbo-pumps. Storing propellants at low pressure reduces tank mass, and this improves the vehicle empty-to-gross mass ratio; if one propellant is responsible for most of the propellant mass (e.g., oxidizer), injecting it while leaving the others solid or pressure-fed can still achieve much of the potential gain. Previously, the principal investigator and his group built and tested ultraminiature-machined micro jet injectors that pumped ethanol and also explored liquid and, more recently, hybrid engine designs. Recent work has focused on designing and implementing a whole-engine test article that simultaneously integrates a steam injector, boiler, decomposition chamber, fuel injector and thrust chamber, that is practical to build, and that is compatible with MEMS fabrication. An axisymmetric engineering mockup in brass was built to demonstrate the feasibility of the design concept (see Figure 1). Configurations that combine electrically-driven pumps with steam injectors by, for example, using electric pumps to pump fuel or coolant and a steam injector motivated by boiled coolant to pump oxidizer are also being explored. These would allow pressurized tanks to be avoided altogether while still being compatible with miniaturization via MEMS.
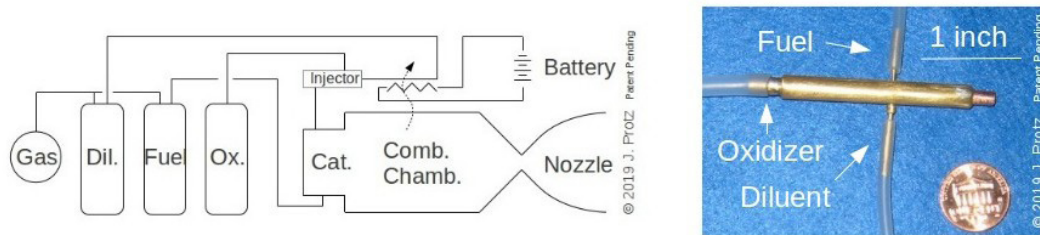
▲ Figure 1: (left) Schematic representation of engine and (right) engineering mock-up in brass of a fully-integrated engine.

FURTHER READING

- J. Protz, "Hybrid and Partially Pressure-Fed Injector-Pumped Micro Rockets," (JANNAF 2019-004BT), presented at the *Joint Army-Navy-NASA-Air Force Joint Meeting of the 13th Modeling and Simulation / 11th Liquid Propulsion / 10th Spacecraft Propulsion Subcommittees and Meeting of the Programmatic and Industrial Base (JANNAF)*, Tampa, FL, Dec. 9-13, 2019.
- J. M. Protz, "Progress Towards an Injector-Pumped Micro Rocket Engine and Vehicle," invited talk to *Gas Turbine Laboratory*, MIT, Cambridge, MA, May 7, 2019.
- J. M. Protz, "Modeling and Analysis of a Giffard-Injector-Pumped Bipropellant Microrocket," invited talk to *Pratt & Whitney Rocketdyne*, Huntsville, AL, February 3, 2010.

Hafnia-filled Photonic Crystal Emitters for Mesoscale Thermophotovoltaic Energy Converters

R. Sakakibara, V. Stelmakh, W.R. Chan, R. Geil, M. Ghebrebrhan, J.D. Joannopoulos, M. Soljačić, I. Čelanović
Sponsorship: ARO, DoE

Thermophotovoltaic (TPV) systems are promising as small scale, portable generators for power sensors, small robotic platforms, and portable computational and communication equipment. In TPV systems, an emitter at high temperature emits radiation that is then converted to electricity by a low bandgap photovoltaic cell. Our group's approach to increase both TPV power and efficiency is to use two-dimensional, hafnia-filled tantalum photonic crystals (PhCs) as emitters. These emitters consist of a 2D array of cylindrical cavities etched in tantalum and filled with hafnia (HfO2). They work by enabling efficient spectral tailoring of thermal radiation for a wide range of incidence angles; they can increase the fuel-to-electricity efficiency of our group's propane-based TPV system from 4.3% to above 12%. However, fabricating these PhCs is difficult: while the deep cavities of the PhC must be filled as completely as possible, using atomic layer deposition to fill the cavities layer by layer leads to an uneven and thick top hafnia surface that adversely impacts the emittance. Because the PhC optical performance improves with a flatter top hafnia surface, we explore methods to planarize the top surface, in particular by depositing a sacrificial oxide layer and etching it back. With a single iteration, the average height difference between the hafnia crest and trough is reduced from about 200nm to 90nm in silicon PhC samples, suggesting a method to fabricate PhCs with improved geometry and emittance. Precise fabrication of PhC emitters can enable high TPV performance and pave the way toward portable micro-generators for off the grid applications.
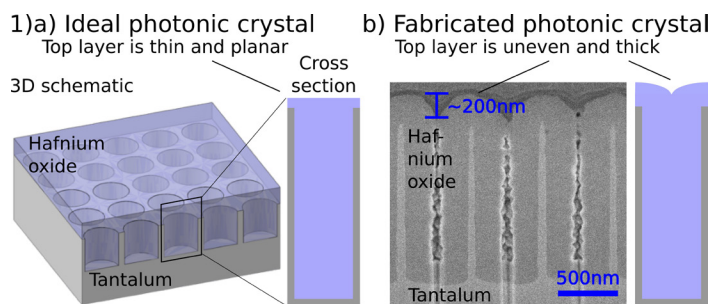
▲ Figure 1: a) Schematic of an ideal filled photonic crystal (PhC) and its cross section, which have a flat and thin top surface. (b) Focused ion beam image of the fabricated filled PhC cross section shows a thick, uneven layer of hafnia above the cavity.

▲ Figure 2: Initial tests of planarization on silicon photonic crystals show a decrease in the height difference between the HfO2 crest and trough.

FURTHER READING

- W. R. Chan, V. Stelmakh, M. Ghebrebrhan, M. Soljačić, J. D. Joannopoulos, and I. Čelanović, "Enabling Efficient Heat-to-electricity Generation at the Mesoscale," *Energy Environ. Sci.*, vol. 10, pp. 1367-1371, 2017.
- Y. X. Yeng, J. Chou, V. Rinnerbauer, Y. Shen, S.-G. Kim, J. D. Joannopoulos, M. Soljačić, and I. Čelanović, "Global Optimization of Omnidirectional Wavelength Selective Emitters/absorbers Based on Dielectric-filled Anti-reflection Coated Two-dimensional Metallic Photonic Crystals," *Opt. Express*, vol. 22, pp. 21711–21718, 2014.
- R. Sakakibara., V. Stelmakh, W. R. Chan, M. Ghebrebrhan, J. D. Joannopoulos, M. Soljačić, and I. Čelanović, "Practical Emitters for Thermophotovoltaics: a Review," *J. Photon. Energy*, vol 9, pp. 032713, 2019.

Fabric Integration of Organic Photovoltaics

M. Saravanapavanantham, J. Mwaura, V. Bulović

In recent years, wearable technologies have emerged as a platform beyond basic functionality, such as a watch or a headphone, into highly integrated tools capable of communications, biosensing, navigation guidance, and performing financial transactions. Yet these technologies remain localized on the body in a bulky form-factor such as a smartwatch, AR glasses, or earbuds. Seamless integration of electronics over large areas into the most indispensable wearable, clothing, remains a distant goal. Forgoing conventional discrete/bulky electronics in place of emerging thin-film alternatives promises to bridge this gap.

In this project, we report integration of organic photovoltaics (OPV) into ultra-lightweight composite fabrics (Dyneema) as a first step towards realizing elec-tronically active fabrics. The devices are fabricated on CVD-deposited ultra-thin dielectric substrates, which lend themselves for use on fabrics through transfer lamination. Employing standard thermal evaporation and RF sputtering processes, we have demonstrated fabric-integrated OPV devices with over 1% power conversion efficiencies. In an effort to realize photovoltaics with higher efficiencies that can power larger electronic devices, we are currently exploring the use of electronic polymer inks, which can be coated/printed through scalable roll-to-roll processes. Techniques developed in this project can also enable integration of other devices including displays, sensors, speakers, and actuators.
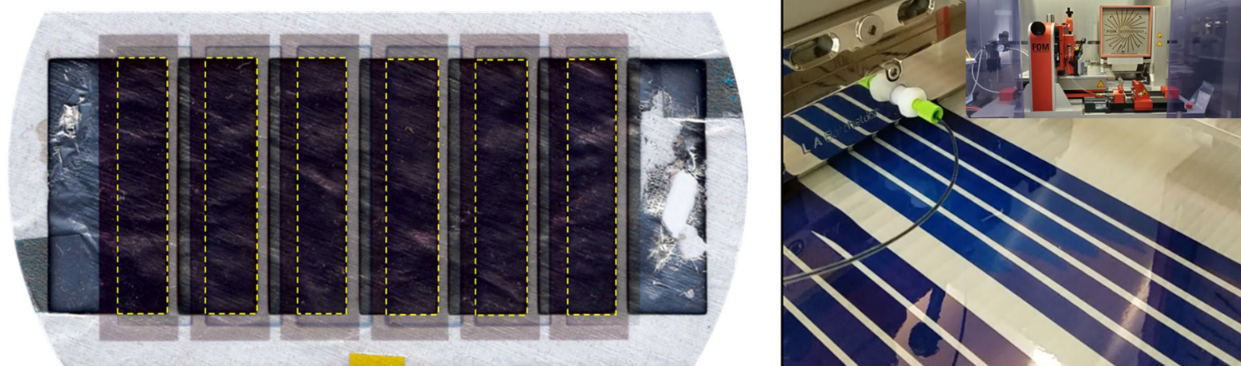
▲ Figure. 1: (Left) Photograph of transfer-laminated organic photovoltaic on Dyneema composite fabric. Active area of the device is outlined in yellow, covering a total area of 13.9 square centimeters. The device has a power conversion efficiency of 1.23%. (Right) Photograph of slot-die coated organic photovoltaic inks being explored to manufacture this technology in a scalable manner at higher power conversion efficiencies. The inset shows a photograph of the slot-die tool housed in MIT.nano.

Balancing Actuation and Computing Energy in Low-power Motion Planning

S. Sudhakar, V. Sze, S. Karaman
Sponsorship: NSF, Cyber-Physical Systems (CPS) Program

We study a novel class of motion planning problems, inspired by emerging low-power robotic vehicles, such as insect-size flyers, high-endurance autonomous blimps, and chip-size satellites for which the energy consumed by computing hardware while planning a path can be as large as the energy consumed by actuation hardware during the execution of the same path. For these new applications, we must consider the total energy of executing and computing a candidate solution to evaluate a motion plan. Figure 1 shows average actuation energy and computing energy curves for a selected robotic platform and computing platform. Here, minimizing only the actuation energy does not minimize the total energy. Instead, stopping computing earlier and accepting a higher actuation energy cost for a lower computing energy cost minimizes the total energy.

We propose a new algorithm, called Computing Energy Included Motion Planning (CEIMP). CEIMP operates similarly to other anytime planning algorithms, except it stops when it estimates further computing will require more computing energy than potential savings in actuation energy. The algorithm relies on Bayesian inference to estimate future energy savings to evaluate the trade-off between the computing energy required to continue sampling and the potential future actuation energy savings after such computation. CEIMP outperforms the average baseline of using maximum computing resources in realistic computational experiments involving 10 MIT building floor plans. On the ARM Cortex-A15, for a simulated vehicle that uses 1 Watt to travel 1 m/s, CEIMP saves 2.1-8.9x the total energy on average across floor plans compared to the baseline, translating to missions that can last 2.1-8.9x longer on the same battery. Figure 2 shows CEIMP in action; while the path returned by CEIMP is longer than the path returned by the baseline, CEIMP's total energy is much closer to the true minimum of total energy than the baseline.
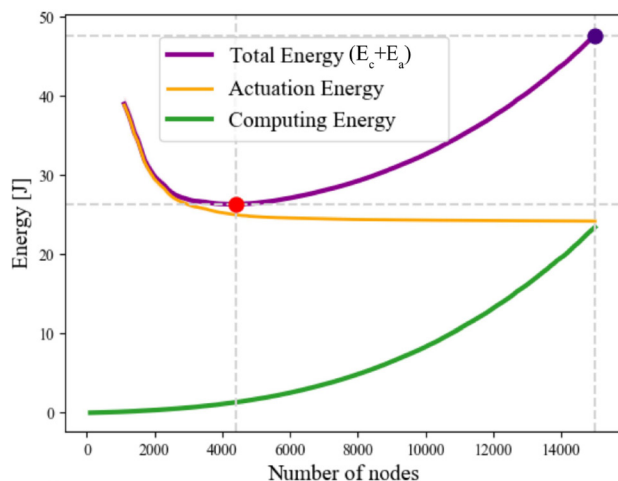
▲ Figure 1: Average computing energy, actuation energy, and total energy (computing + actuation) curves vs. nodes in PRM*, a sampling-based motion planner.
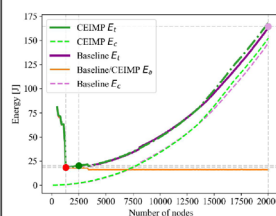
(a) Energy curves vs. n

(b) Path returned by CEIMP
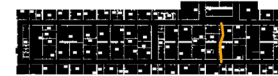
(c) Path returned by baseline

▲ Figure 2: Energy curves vs. nodes in PRM* for a single trial and paths returned by CEIMP and the baseline. True minimum of total energy curve (red marker), baseline total energy (purple marker), and CEIMP total energy (green marker) are marked.

FURTHER READING

- S. Sudhakar, S. Karaman, and V. Sze, "Balancing Actuation and Computing Energy in Motion Planning," presented at *International Conference on Robotics and Automation (ICRA)*, Paris, France, 2020.

Enabling Low-cost Electrodes in PbS Solar Cells through a Nickel Oxide Buffer Layer

E. Wassweiler, M. Sponseller, J. Jean, A. Osherov, M. Bawendi, V. Bulović
Sponsorship: NSF GRFP, Tata-GridEdge Solar

The versatile characteristics of lead sulfide quantum dots (PbS QD) make them an attractive material to develop high-efficiency, low-cost, and flexible photovoltaics (PVs). Hole transport layers (HTLs) and electron transport layers are essential building blocks in these solar cell architectures. PbS QDs with an EDT ligand are widely used as an HTL in high-efficiency QDPVs. However, the limited compatibility of the EDT with different electrode materials prevents the continued development of QDPVs into manufacturing capable device architectures. Specifically, the dependence on gold electrodes is cost-prohibitive for depositing QDPVs on a large scale.

While gold cannot be used on a commercial scale, less expensive but more chemically reactive materials can be used. Replacing gold with aluminum or copper would cut material costs by a factor of at least 1,200.

Through the use of a nickel oxide (NiOx) buffer layer, these devices become compatible with lower-cost electrodes. As a p-type metal oxide, NiOx is a favorable HTL material with a high work function, large band gap, and film stability.

In fact, through the use of a NiOx buffer layer, power conversion efficiencies for devices with lower-cost electrodes are equivalent to their gold electrode counterparts. However, even though NiOx buffer layer devices show improved performance and stability compared to devices without NiOx buffer layers, the power conversion efficiency drops after a couple of months due to a new barrier within the device stack. Current research focuses on improving the stability of QDPVs with low cost electrodes through identifying and mitigating the barrier formation.
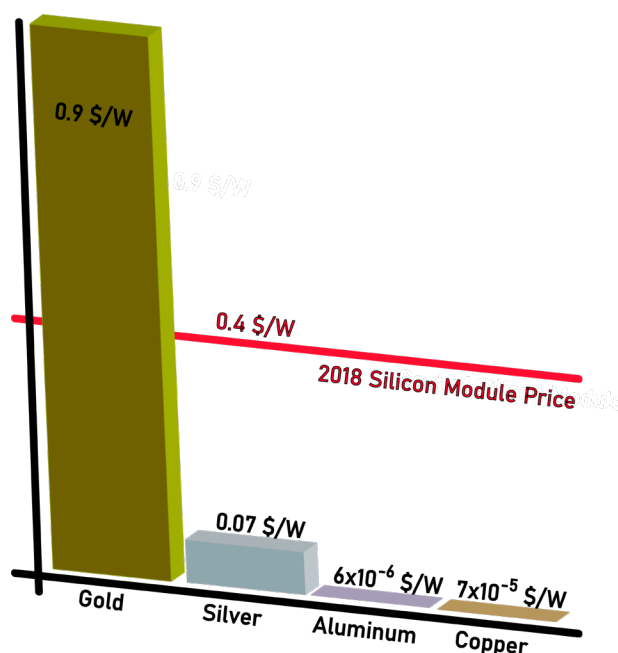
▲ Figure 1: Cost associated with different electrode materials.
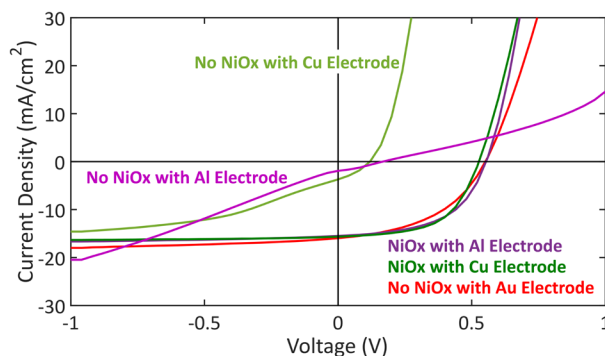
▲ Figure 2: Comparison of JV curves between solar cells with gold and aluminum electrodes.

FURTHER READING

- E. L. Wassweiler, "Engineering Scalable Device Architectures for Lead Sulfide Quantum Dot Solar Cells," *Master's Thesis*, Massachusetts Institute of Technology, Cambridge, 2019.

Architecture-level Energy Estimation of Accelerator Designs

Y. N. Wu, J. S. Emer, V. Sze

With Moore's law slowing down and Dennard scaling ending, energy-efficient domain-specific accelerators have become a promising direction for hardware designers to continue bringing energy efficiency improvements to data and computation intensive applications. To ensure fast exploration of accelerator design space, architecture-level energy estimators, which perform energy estimations without requiring complete hardware description of the designs, are critical to designers. However, it is hard to use existing architecture-level energy estimators to obtain accurate estimates for accelerator designs, as accelerator designs are diverse and sensitive to data patterns.

To solve this problem, we present Accelergy (Figure 1), an architecture-level energy estimation methodology. Accelergy allows the users to define their own components in their designs to allow descriptions of the diverse design space. At the same time, to reflect the energy differences brought by special data patterns, e.g., sparsity in data, Accelergy also allows the users to define special actions types related to the components. To enhance flexibility, Accelergy defines an interface to communicate with other estimators that focus on energy estimations of specific types of components in the designs (e.g., memory storage components). To illustrate the usage of Accelergy methodology, we implemented an example framework for energy estimations of deep neural network (DNN) accelerator designs. We further integrate Accelergy with Timeloop, a DNN mapping space exploration tool, to enable accurate estimation of processing-in-memory (PIM) based DNN accelerator designs. We validated the Accelergy framework on a conventional digital design Eyeriss as well as a PIM-based design, both achieving a total energy estimation accuracy of 95% and accurate energy breakdowns of various components in the designs (Figure 2).
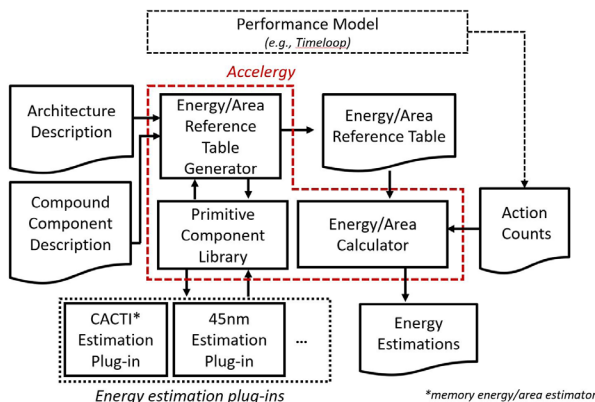
▲ Figure 1: System diagram of Accelergy. Accelergy takes in design description and run time action counts as inputs and generates the energy estimation as the output.
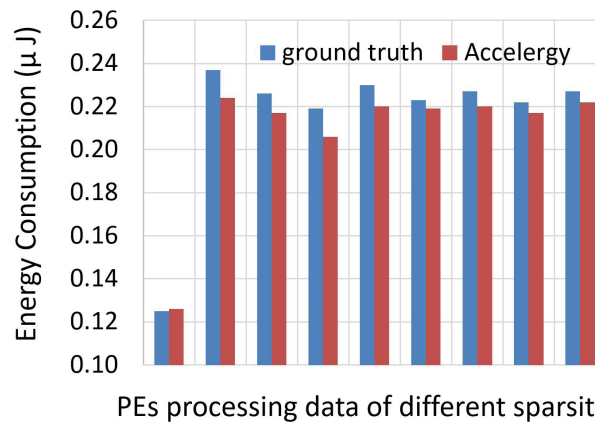
▲ Figure 2: Energy estimation comparison on the energy breakdown across the PEs, each of which processes data of a different sparsity, in Eyeriss PE array (only selected PE are shown).

FURTHER READING

- Y. N. Wu, J. S. Emer, and V. Sze, "Accelergy: An Architecture-Level Energy Estimation Methodology for Accelerator Designs," *ICCAD*, 2019.
- Y. N. Wu, V. Sze, and J. S. Emer, "An Architecture-Level Energy and Area Estimator for Processing-In-Memory Accelerator Designs," *ISPASS*, 2020.
- A. Parashar, P. Raina, Y. S. Shao, Y.-H. Chen, V. A. Ying, A. Mukkara, R. Venkatesan, B. Khailany, S. W. Keckler, and J. Emer, "Timeloop: A Systematic Approach to DNN Accelerator Evaluation," *ISPASS*, 2019.

Low-frequency Buckled Beam MEMS Energy Harvester

R. Xu, H. Akay, Z. Lian, H. Li, S.-G. Kim
Sponsorship: MIT-SUTD International Design Center

Vibrational energy harvesting at the MEMS scale is a unique challenge for low-frequency sources which are ubiquitous but do not operate at resonant frequencies of structures on the micro scale. It is nature's law that resonant frequency is inversely proportional to mass, which is a great challenge for micro-scale energy harvesting devices operating at low frequencies (less than 100Hz). A bi-stable buckled beam design is presented that does not rely on resonance of a MEMS structure but rather operates by snapping between buckled states at low frequencies.

A fully functional piezoelectric MEMS energy harvester is designed, monolithically fabricated, and tested. An electromechanical lumped parameter mod-el is developed to analyze the nonlinear dynamics and to guide the design of the nonlinear oscillator-based energy harvester. Multi-layer beam structure with residual stress induced buckling is achieved through the progressive residual stress control of the deposition processes along the fabrication steps. Dynamic testing, however, demonstrated that optimizing the beam stiffness to proof mass ratio was challenging given the presence of undesired modes of vibration. A new iteration of the design was fabricated with changes to the proof mass geometry which stabilize the oscillations by reducing rotational inertia, a key variable in enhancing dynamic performance of the device.
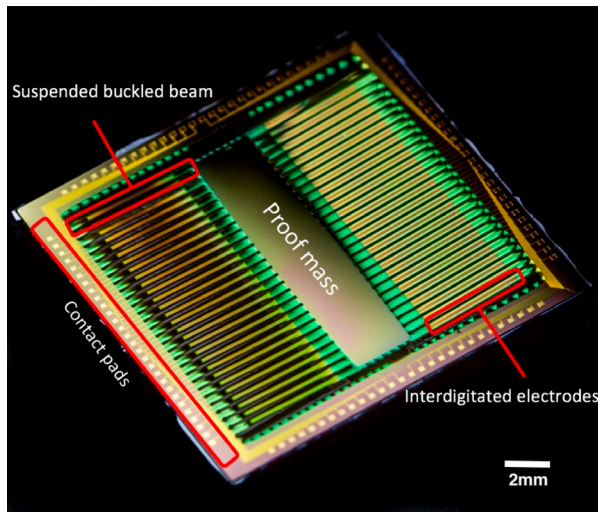
▲ Figure 1: Photograph of released buckled beam energy harvesting device.
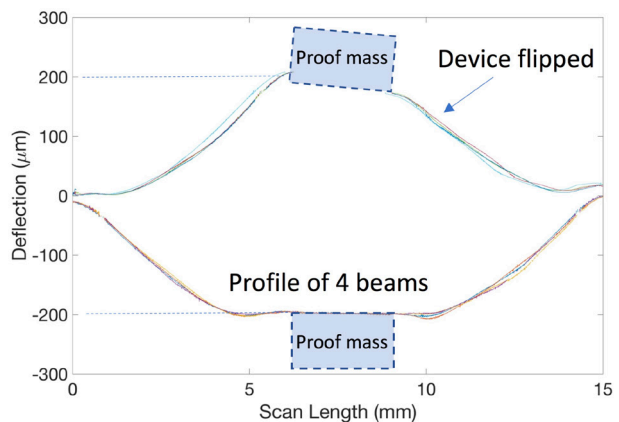
▲ Figure 2: Surface profile of four beams displaying buckling on both sides.

FURTHER READING

- R. Xu, H. Akay, and S.-G. Kim, "Buckled MEMS Beams for Energy Harvesting from Low Frequency Vibrations," Research, 2019, 1087946.
- R. Xu, "Low-Frequency, Low-Amplitude MEMS Vibration Energy Harvesting," Doctoral Thesis, Massachusetts Institute of Technology, 2018.
- R. Xu S.-G. Kim, "Modeling and Experimental Validation of Bi-Stable Beam Based Piezoelectric Energy Harvester," Energy Harvesting and Systems, 1;3(4):313-21, Oct. 2016.

A CMOS-based Energy Harvesting Approach for Laterally-arrayed Multi-bandgap Concentrated Photovoltaic Systems

H. Zhang, K. Martynov, D. J. Perreault
Sponsorship: ARPA-E

When high solar conversion efficiency is desired, people often adopt concentrated photovoltaic systems with multi-junction cells. However, traditional tandem structures widely used in such systems can suffer from current-mismatch effects with spectrum variations, whereas the Laterally-Arrayed Multi-Bandgap (LAMB) cell structure is a potentially higher-efficiency and lower-cost alternative.

Here we show an energy harvesting approach designed to take full advantage of the LAMB cell structure. Individual cells within a sub-module block are connected for approximate voltage-matching, and a Multi-Input Single-Output (MISO) buck converter combines the energy and performs Maximum Power Point Tracking locally. A miniaturized MISO dc-dc converter prototype is developed in a 130nm CMOS process. For 45-160mW power levels, >95% peak efficiency is achieved in a small form factor designed to fit within available space in a LAMB cell block. The results demonstrate the potential of the LAMB CPV system for enhanced solar energy capture.
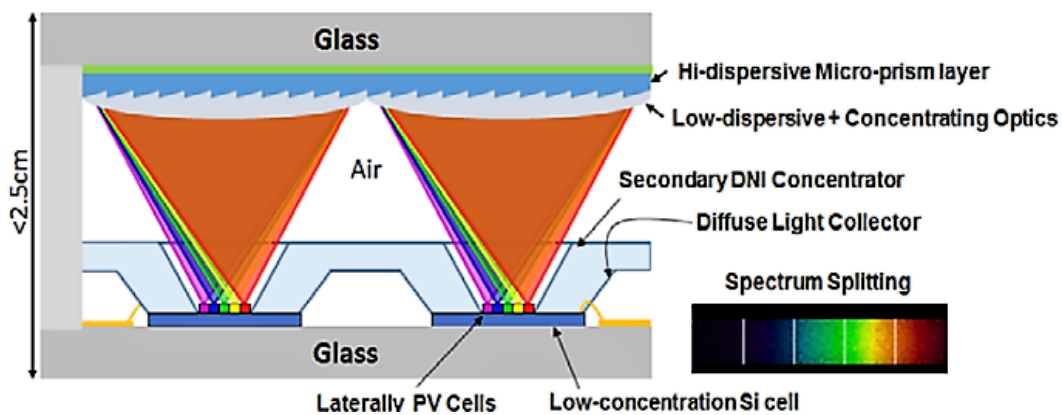
▲Figure 1: Structure of a LAMB cell unit. An optical layer spectrally-splits and focuses direct sunlight onto multi-bandgap III-V cells, and a Si cell collects diffuse light.
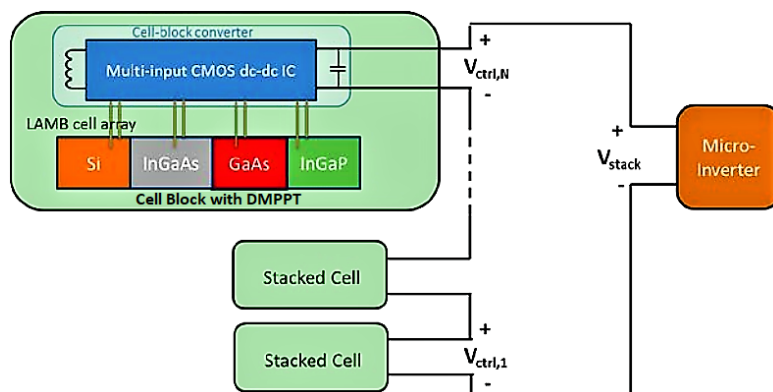
◀Figure 2: Proposed power management structure. Each cell block comprises several LAMB cell units, and a dc-dc converter that tracks local maximum power point and combines energy generated from multiple cells into a single output. The power from individual converters can then be combined, e.g. by stacking in series.

FURTHER READING

- H. Zhang, K. Martynov, and D. J. Perreault, "A CMOS-Based Energy Harvesting Approach for Laterally-Arrayed Multi-Bandgap Concentrated Photovoltaic Systems," in *IEEE Transactions on Power Electronics*.
- H. Zhang, K. Martynov, D. Li, R. Wen, J. Michel, and D. J. Perreault, "A Power Management Approach for Laterally-Arrayed Multi-Bandgap Concentrated Photovoltaic Systems," *2019 IEEE 46th Photovoltaic Specialists Conference (PVSC)*, Chicago, IL, USA, 2019, pp. 0702-0707.
- D. Li, et al., "Spectrum Splitting Micro-Concentrator Assembly for Laterally-arrayed Multi-Junction Photovoltaic Module," *2018 Conference on Lasers and Electro-Optics (CLEO)*, San Jose, CA, 2018, pp. 1-2.